

Iterative Channel Decoding of FEC-Based Multiple-Description Codes

Seok-Ho Chang, *Member, IEEE*, Pamela C. Cosman, *Fellow, IEEE*, and Laurence B. Milstein, *Fellow, IEEE*

Abstract—Multiple description coding has been receiving attention as a robust transmission framework for multimedia services. This paper studies the iterative decoding of FEC-based multiple description codes. The proposed decoding algorithms take advantage of the error detection capability of Reed–Solomon (RS) erasure codes. The information of correctly decoded RS codewords is exploited to enhance the error correction capability of the Viterbi algorithm at the next iteration of decoding. In the proposed algorithm, an intradescription interleaver is synergistically combined with the iterative decoder. The interleaver does not affect the performance of noniterative decoding but greatly enhances the performance when the system is iteratively decoded. We also address the optimal allocation of RS parity symbols for unequal error protection. For the optimal allocation in iterative decoding, we derive mathematical equations from which the probability distributions of description erasures can be generated in a simple way. The performance of the algorithm is evaluated over an orthogonal frequency-division multiplexing system. The results show that the performance of the multiple description codes is significantly enhanced.

Index Terms—Cross-layer design, iterative decoding, multimedia communications, multiple description coding, orthogonal frequency-division multiplexing (OFDM), progressive transmission, wireless video.

I. INTRODUCTION

THE GROWING demand for multimedia services has motivated intense research on cross-layer design [1], which is particularly important for transmission over mobile radio channels. Advances in source codecs such as progressive image or scalable video coders [2]–[4] employ a progressive mode of transmission such that as more bits are received, the source can be reconstructed with better quality. However, these advances have also rendered the encoded bitstreams very sensitive

Manuscript received February 17, 2011; revised June 08, 2011 and September 03, 2011; accepted September 14, 2011. Date of publication September 29, 2011; date of current version February 17, 2012. This work was supported in part by Intel Corporation, by Cisco Systems, Inc., and by the National Science Foundation under Grant CCF-0915727. The associate editor coordinating the review of this manuscript and approving it for publication was Dr. Charles Creusere.

S.-H. Chang was with the Department of Electrical and Computer Engineering, University of California, San Diego, La Jolla, CA 92093-0407 USA. He is now with Qualcomm Inc., San Diego, CA 92121-1714 USA (e-mail: seokhoc@qualcomm.com).

P. C. Cosman and L. B. Milstein are with the Department of Electrical and Computer Engineering, University of California, San Diego, La Jolla, CA 92093-0407 USA (e-mail: pcosman@ucsd.edu; milstein@ece.ucsd.edu).

Color versions of one or more of the figures in this paper are available online at <http://ieeexplore.ieee.org>.

Digital Object Identifier 10.1109/TIP.2011.2169973

to channel impairments, which can be severe in mobile channels. Early studies [5], [6] considered the transmission of a progressively compressed bitstream using rate-compatible punctured convolutional (RCPC) codes. Coding and diversity are effective techniques for improving the transmission reliability. However, time diversity achieved by channel coding becomes less effective in a slow fading channel where prolonged deep fades often result in the erasure of the whole packet [6].

Multiple description source coding has emerged as an attractive framework for robust multimedia transmission over packet erasure channels [7]. The basic idea is to generate multiple descriptions of the source such that each description independently describes the source with certain fidelity. When more than one description is available, they can be combined to enhance the quality [8]. Due to the individually decodable nature of the descriptions, the loss of some descriptions does not jeopardize the decoding of correctly received descriptions. Earlier studies of multiple description coding concentrated on information-theoretic bounds for specific input source models [9], [10]. However, recently, the practical implementation of multiple description coding has received attention [7] (the references therein); FEC-based multiple description coding has become popular [11]–[14] since it is flexible in generating arbitrary numbers of descriptions from a progressive bitstream, compared with a source-coder-based approach. In [15]–[19], FEC-based multiple description coding is employed for the transmission of the progressive bitstream against deep fades in a wireless channel. In this scheme, contiguous information symbols from the progressive bitstream are spread across multiple packets. The information symbols are protected against error using a systematic Reed–Solomon (RS) erasure code across multiple descriptions (i.e., packets), and the level of protection is determined depending on the relative importance of the information symbols, which is referred to as unequal error protection (e.g., see Fig. 1). After RS erasure encoding, each description is encoded by a concatenation of an outer cyclic redundancy code (CRC) and an inner RCPC code. The CRC allows the channel to be treated as an erasure channel. These schemes can be viewed as product channel codes, where the RS code is employed as a column code and where the concatenation of the CRC and the RCPC code is employed as a row code.

Another popular transmission scheme for a progressive source, proposed in [20], is also based on product codes. It received attention due to its robust performance in a mobile fading channel. The product codes in [20] also employ a systematic RS erasure code across multiple packets (i.e., a column code) and a concatenation of CRC and the RCPC code

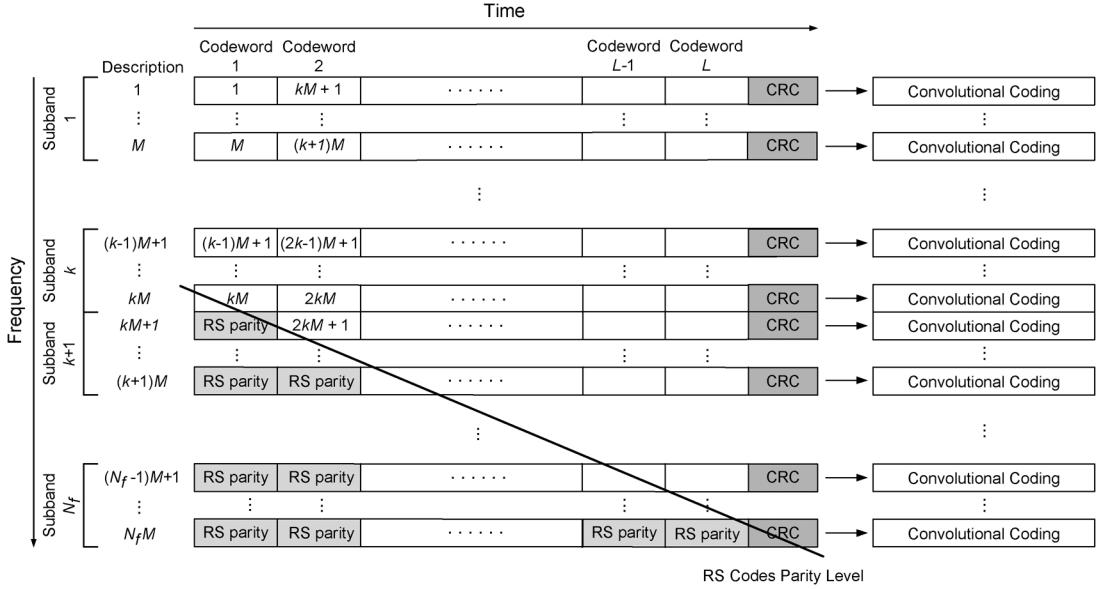


Fig. 1. Multiple description codes in an OFDM frame.

to encode each packet (i.e., a row code). However, unlike the multiple description codes, the system in [20] does not allow an arbitrary set of packets to be lost since it puts the earliest contiguous progressive bits in the same packets. That is, the system in [20] is sensitive to the location of erasures in a series of packets. The performance evaluation in [16] shows that FEC-based multiple description codes outperform the product code in [20], whereas the latter exhibits less delay in decoding of the source.

We study the iterative decoding of FEC-based multiple description codes. Considering the progress in very large scale integration technology (VLSI), which allows more complex decoding, and the growing demand for progressive multimedia services, it is interesting to study the performance of a popular progressive transmission scheme, i.e., multiple description codes, using iterative decoding algorithms. Srinivasan [21] studied iterative decoding of multiple description source coding, which is a source-coder-based approach used to generate multiple correlated descriptions of a source. Multiple description source encoding produces two correlated bitstreams (i.e., descriptions), and each description is separately encoded using a convolutional encoder. Exploiting the correlation between the two descriptions, at the receiver, the iterative decoding algorithm used for turbo codes [22] is employed. On the other hand, this paper studies iterative decoding of FEC-based multiple description coding, which has different encoder and decoder structures from those of a source-coder-based approach. Sun *et al.* [23] combined FEC-based multiple description coding with differential space-time codes [24], which is used for multiple-input multiple-output antenna (MIMO) systems. For the combined system, Sun *et al.* suggested iterative decoding using both the convolutional decoder and the differential space-time decoder (note that the FEC-based multiple description codes consist of outer RS erasure codes and inner convolutional codes). At the receiver, the two decoders (i.e., the convolutional decoder and the differential space-time decoder) exchange soft information (*a priori* probabilities) between themselves

in successive iterations, such as turbo decoding. After the last iteration is completed, CRC and RS decoding is performed for the final output of the convolutional decoder to recover the source bitstream.

In this paper, we propose iterative decoding algorithms that take advantage of the error detection capability of RS erasure codes. The correctly decoded hard-decision results of systematic RS decoding are exploited as known correct information bits for the Viterbi algorithm in the subsequent iteration of decoding. An important feature of the proposed algorithm is the use of an intrapacket (i.e., intradescription) interleaver, which is placed between the outer RS codes and inner convolutional codes. The purpose of this interleaver is to distribute the known correct information bits uniformly over a description for the Viterbi decoder in the subsequent iteration. This differs from the conventional outer interleaver, which is often used in the concatenated codes of outer RS and inner convolutional codes. We also address the optimization of RS code parity levels. Determining the number of parity symbols for each RS codeword, related with unequal error protection, is a key design problem in multiple description coding [16]. For the optimization of RS code parity levels in iterative decoding, we derive mathematical equations from which the probability distributions of the correctly decoded descriptions can be calculated.

Note that there are some significant differences between [23] and this paper. Sun *et al.* combined FEC-based multiple description coding with a specific MIMO coding (differential space-time codes) and performed iterative decoding using the convolutional decoder and the differential space-time decoder. On the other hand, this paper does not assume either a specific modulation or MIMO coding and is purely focused on the FEC-based multiple description codes themselves: the source bitstream is iteratively decoded using two constituent decoders (i.e., an RS erasure decoder and a convolutional decoder combined with a CRC decoder) of the multiple description codes.

The proposed iterative decoding structure is a general one that can be applied to any FEC-based multiple description

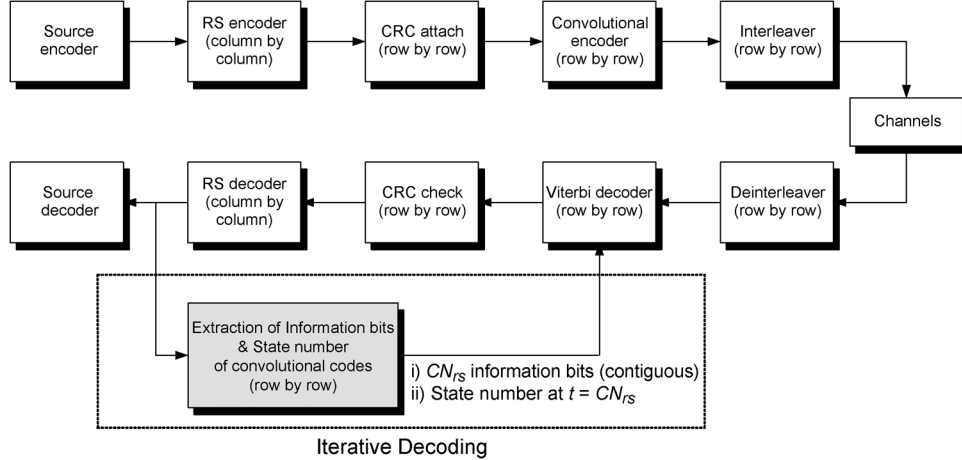


Fig. 2. Iterative channel decoding scheme I.

system. In this paper, as an example application, orthogonal frequency-division multiplexing (OFDM) is considered. OFDM is used in many current applications, and the use of multiple description codes over OFDM systems has been of interest [17]–[19], [25]–[27]. The numerical evaluations show that the performance of the multiple description codes can be significantly improved if the proposed iterative decoding algorithm is employed, and RS parity levels are appropriately optimized based on our method. The rest of this paper is organized as follows. In Section II, we provide the system model and technical preliminaries. In Section III, the proposed iterative decoding algorithms are described. In Section IV, the optimization of RS code parity levels for unequal error protection is presented. In Section V, numerical results and discussions are provided, and we conclude this paper in Section VI.

II. SYSTEM MODEL

We first describe the channel model for the OFDM system considered in [17]–[19] and [25]. OFDM splits a high-rate data stream into a number of lower rate data streams that are transmitted over orthogonal subcarriers. The total number of subcarriers is denoted by N_s . It is assumed that a frequency-selective fading environment has N_f independent fading subbands, and each of the N_f subbands consists of M highly correlated subcarriers (i.e., $N_s = N_f M$). Let $s[n, u, v]$ be the v th input modulated symbol of a packet (i.e., description)¹ at the u th subcarrier in the n th subband. Let V denote the description size in terms of the modulated symbols. At the receiver, the output signal $r[n, u, v]$ can be expressed as

$$r[n, u, v] = \alpha[n, u, v]s[n, u, v] + w[n, u, v], \\ \text{for } 1 \leq n \leq N_f, 1 \leq u \leq M, 1 \leq v \leq V \quad (1)$$

where $\alpha[n, u, v]$ is a zero-mean complex-valued Gaussian random variable with a Rayleigh-distributed envelope. It is assumed that the zero-mean complex Gaussian noise $w[n, u, v]$ is independent for different n , u , and v values. Since the subcarriers within a channel are highly correlated, we have

$$\alpha[n, u, v] \approx \alpha[n, v]. \quad (2)$$

¹In this paper, each packet corresponds to a single description. Hence, in what follows, we will use the terms “packet” and “description” interchangeably.

This corresponds to the widely used block fading channel model [28]–[30] in the frequency domain. Fig. 1 shows multiple description codes in an OFDM frame. The contiguous progressive source bits are first grouped into RS code symbols, where each RS symbol consists of N_{rs} bits (i.e., RS code symbols belong to $\text{GF}(2^{N_{rs}})$). In the frequency domain, N_s descriptions of approximately equal importance are constructed, where contiguous RS information symbols are spread across the multiple descriptions. The information symbols are protected by systematic (N_s, k) RS erasure codes with the level of protection depending on the relative importance of the information symbols ($1 \leq k \leq N_s$). This RS erasure code can correct up to $N_s - k$ erasures [31]. We let L denote the description size in terms of RS code symbols, and let r_l denote the number of information symbols assigned to the RS codeword l ($1 \leq l \leq L$). As the compressed bitstream has different sensitivities toward channel errors, the system performance is improved by employing unequal error protection. Error protection decreases for the RS codewords as we move to the right, i.e., $r_1 \leq r_2 \leq \dots \leq r_L$ [15]–[19], as shown in Fig. 1. After RS encoding, a concatenation of CRC and RCPC codes is applied to each description for possible diversity and coding gains in the time domain. Since all the descriptions are approximately equally important, RCPC codes with the same code rate can be applied to protect each individual description [16], [19]. Lastly, the individual descriptions are mapped to the N_s subcarriers of an OFDM frame. After RCPC decoding, the CRC is used to erase any description with bit errors. The subsequent RS decoding operates in an erasure-only mode. It should be noted that the performance of the system only depends on the number of erasures in N_s descriptions and is insensitive to the location of erasures.

III. PROPOSED ITERATIVE DECODING ALGORITHM

To begin with, we present the procedure of noniterative decoding [16], [19], which is depicted in Fig. 2, if one ignores the shaded block used for iterative decoding. The deinterleaver conventionally deinterleaves bits within each description such that fades introduced by the channel are spread within a description, which allows a convolutional code to perform well in the presence of bursty errors. A Viterbi decoder performs soft decoding

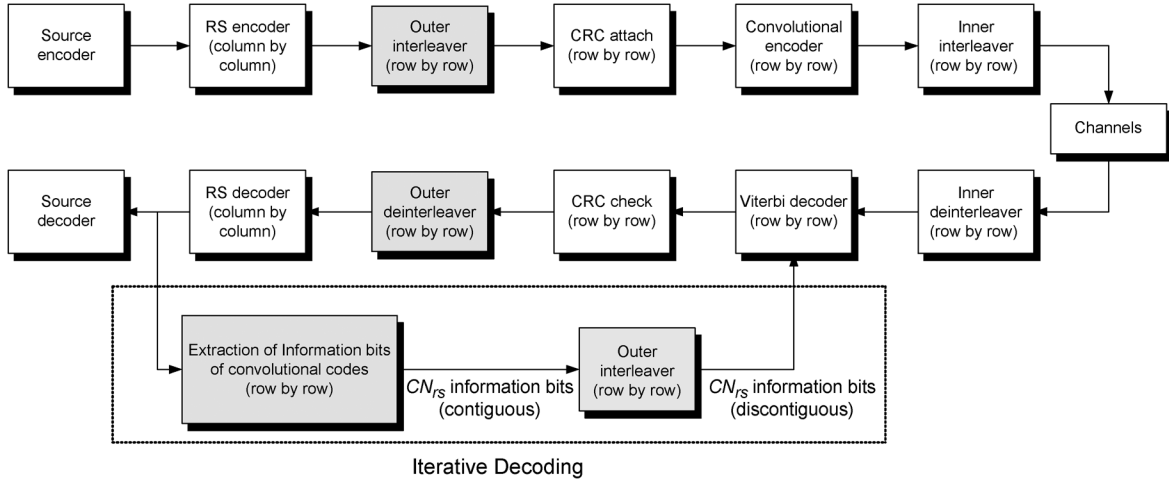


Fig. 3. Iterative channel decoding scheme II.

of each of N_s descriptions and makes hard decisions on decoded bits. A CRC decoder detects whether each description contains bit errors. A description having any bit errors, referred to as an erroneous description, is declared an erasure for RS decoding. As stated before, for RS codeword l having $N_s - r_l$ parity symbols ($1 \leq l \leq L$), the RS decoder can correct up to $N_s - r_l$ erasures. Since we have $r_1 \leq r_2 \leq \dots \leq r_L$ due to unequal error protection, the correctly decoded RS codewords (i.e., columns in the product code) would be placed contiguously at the left end of the product code. Let C denote the number of correctly decoded RS codewords. Then, it can be shown that the number of erroneous descriptions after Viterbi decoding, which is denoted by N_e , is in the following range:

$$N_s - r_{C+1} < N_e \leq N_s - r_C. \quad (3)$$

We now describe iterative decoding scheme I, which is shown in Fig. 2. From the hard-decision results of RS decoding with the error detection capability, we know that there are CN_{rs} contiguous correct bits at the left end of each description, where N_{rs} is the number of bits per RS code symbol. Note that in Figs. 1 and 2, these bits correspond to the first CN_{rs} information bits of each convolutional code. Since we know both the first CN_{rs} information bits as well as the starting state in the trellis diagram (i.e., the state at $t = 0$), the state at $t = CN_{rs}$ can be calculated. With this information, in the subsequent iteration, the Viterbi algorithm redecodes the descriptions received from the channels. The first CN_{rs} information bits do not need to be decoded. Only the remaining $(L - C)N_{rs}$ information bits are decoded using the known state at $t = CN_{rs}$. As a result, the redecoded description consists of the first CN_{rs} correct bits and the remaining $(L - C)N_{rs}$ bits that are redcoded. The CRC decoder again checks whether there is any bit error in each redecoded description. If some bit errors in the erroneous descriptions are corrected, the number of erroneous descriptions may decrease. In this case, the RS decoder sees fewer erasures than in the previous iteration; hence, more progressive source bits can be recovered from RS decoding.

We present the iterative decoding scheme II depicted in Fig. 3. The difference from scheme I is the use of an outer

interleaver, which performs bit-level intrapacket (i.e., intradescription) interleaving. This differs from the conventional outer interleaver, which is often used in the concatenated codes of the outer RS and inner convolutional codes [31]–[34] (the differences are summarized at the bottom of this paragraph). After CRC decoding, the data within each description are intradescription deinterleaved by the outer deinterleaver at the receiver side in Fig. 3. Since each description has already been classified into erroneous or correct description by the CRC decoder, deinterleaving does not change the number of erasures. Consequently, the use of an outer interleaver/deinterleaver in Fig. 3 does not improve the performance of noniterative decoding. In the subsequent iteration, however, the outer interleaver at the receiver side interleaves the first CN_{rs} correct information bits of each convolutional code before they are offered to the Viterbi decoder. As a result, the Viterbi algorithm will exploit CN_{rs} correct information bits, which are not contiguous in general. In the following, we describe the differences between the proposed and the conventional outer interleavers. First, residual errors after Viterbi decoding are known to be bursty even for an additive white Gaussian noise (AWGN) channel. The conventional outer interleaver in the concatenated codes spreads those bursty errors across multiple packets so that the RS code can operate with memoryless errors. However, the outer interleaver in Fig. 3 performs intrapacket interleaving and thus has nothing to do with the spreading of bursty errors for the RS code. Note that the system in Fig. 1 has already employed a product code structure so that the RS decoder can combat bursty errors [31]. Second, the use of an outer interleaver in Fig. 3 does not improve the performance of noniterative decoding but only affects the performance of iterative decoding. This differs from the case of the conventional outer interleaver in the concatenated codes. Third, the outer interleaver in Fig. 3 performs bit-level interleaving. The conventional outer interleaver in the concatenated codes performs RS symbol-level interleaving so as to prevent a burst of only two bit errors after Viterbi decoding from spoiling two RS symbols [32]–[34].

In the following, for both decoding schemes I and II, we present how the known correct information bits of a convolutional code can be used to achieve better decoding performance

of other information bits. Consider decoding scheme I shown in Fig. 2. As stated before, from the first CN_{rs} correct information bits, the state at $t = CN_{rs}$ can be calculated. As an example, consider a convolutional code that has the constraint length K and rate $1/n$. This code has 2^{K-1} states in the encoder state diagram, and there are 2^K possible branches between the nodes at $t = t_1$ and $t = t_1 + 1$ in the trellis diagram. Suppose that we know the state in the node at $t = t_1$. Then, we can reduce 2^K candidate branches connecting the nodes at $t = t_1$ and $t = t_1 + 1$ to two because there are only two branches which diverge from a specific state at $t = t_1$. This can prevent wrong trellis paths with small path metrics from being selected as a survival path when the decoder traces back the trellis paths [31], [35]. Consider decoding scheme II shown in Fig. 3. As stated before, CN_{rs} correct information bits are dispersed by the outer interleaver at the receiver side, and thus they are not contiguous in general. We again consider a convolutional code with the constraint length K and with rate $1/n$. Suppose that we know one input information bit at the state transition between $t = t_1$ and $t = t_1 + 1$ in the trellis diagram. Then, 2^K candidate branches between the nodes at $t = t_1$ and $t = t_1 + 1$ can be limited to 2^{K-1} branches. Similar to the case when the state is known to the Viterbi algorithm, this can also prevent wrong trellis paths from being chosen as a survival path [36]–[38]. We note that the outer interleaver at the transmitter side in Fig. 3 should perform the same interleaving pattern that the outer interleaver at the receiver side does. For example, suppose that the Viterbi algorithm is informed of one input information bit at the state transition between $t = t_1$ and $t = t_1 + 1$ after the outer interleaving is performed at the receiver. In addition, suppose that the outer interleaver at the transmitter side performed a different interleaving pattern. Then, the received n convolutional coded bits, which correspond to the known input information bit, would not be placed at the state transition between $t = t_1$ and $t = t_1 + 1$ in the trellis diagram.

In the following, we numerically evaluate how much the decoding performance of other information bits can benefit from the known correct information bits. A convolutional code with a rate of $1/2$, constraint length $K = 7$, and polynomials $(133, 171)$ in octal is employed over an AWGN channel [39]. RS code symbols are from $\text{GF}(2^8)$ (i.e., $N_{rs} = 8$), and the description size in terms of RS code symbols is 32 (i.e., $L = 32$). We assume that two RS codewords are correctly decoded (i.e., $C = 2$), and thus 16 correct information bits are known to the Viterbi algorithm in the subsequent iteration. Note that as $LN_{rs} = 256$, the total number of information bits in a convolutional code (or description) is 256. We first evaluate decoding scheme I. The state in the node at $t = 16$ can be calculated and is known to the Viterbi algorithm. Fig. 4(a) depicts the resultant probability of bit errors at each position in the convolutional code. It should be noted that the low error probabilities at the right are due to the $K - 1$ tail bits in a convolutional code. Fig. 4(a) shows that the known state at $t = 16$ improves the decoding performance of some other information bits at the left. From our observations, the number of those bits is on the order of the constraint length of a convolutional code.

We next evaluate decoding scheme II. Suppose that, to begin with, only one correct information bit is known to the Viterbi

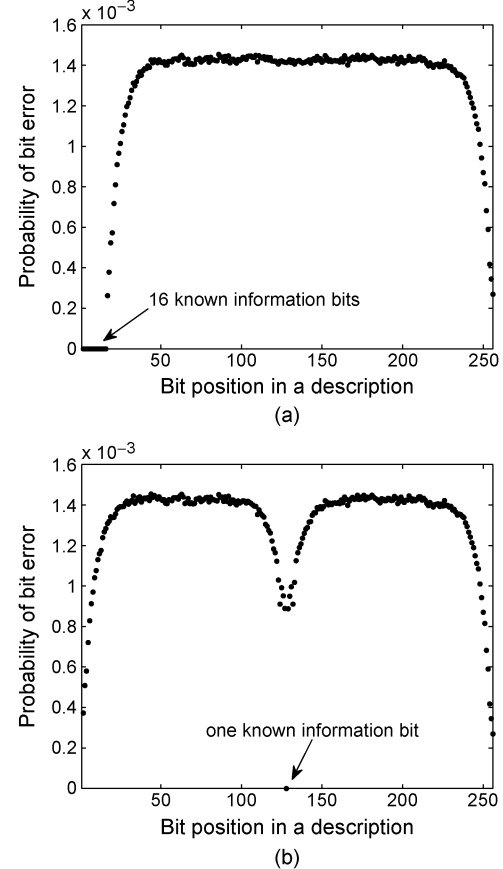


Fig. 4. Probability of bit errors at each position in a description (packet). (a) Sixteen contiguous information bits placed at the left are known to the Viterbi algorithm. (b) One information bit is known to the Viterbi algorithm.

algorithm in the subsequent iteration. In addition, suppose that the known bit is the input at the transition between $t = 127$ and $t = 128$ in the trellis diagram. Fig. 4(b) depicts the resultant probability of bit errors at each position in a convolutional code (or description). Note that the low error probabilities at the left and the right are due to the $K - 1$ initial and tail bits in a convolutional code. Fig. 4(b) shows that, with a single known information bit, the decoding performance of other information bits improves. From our observations, the number of those bits is on the order of the constraint length of a convolutional code. Now, assume that 16 correct information bits, i.e., randomly dispersed by the outer interleaver in Fig. 3, are given to Viterbi algorithm. An example is depicted in Fig. 5(a). Compared with the case of decoding scheme I shown in Fig. 4(a), more decoded bits show improved error probabilities. Note that if a decoded description contains even one bit error, it is declared an erasure for RS erasure decoding. We intend to use an outer interleaver, which spreads known correct information bits uniformly over a description, so that the decoding performance of a large number of bits in a description improves. Regarding the design of the outer interleaver, note that the encoder does not know how many RS codewords will be correctly decoded at the receiver, i.e., how many correct information bits will be interleaved and provided to the Viterbi algorithm in the subsequent iteration. The only thing the encoder knows is that the correct

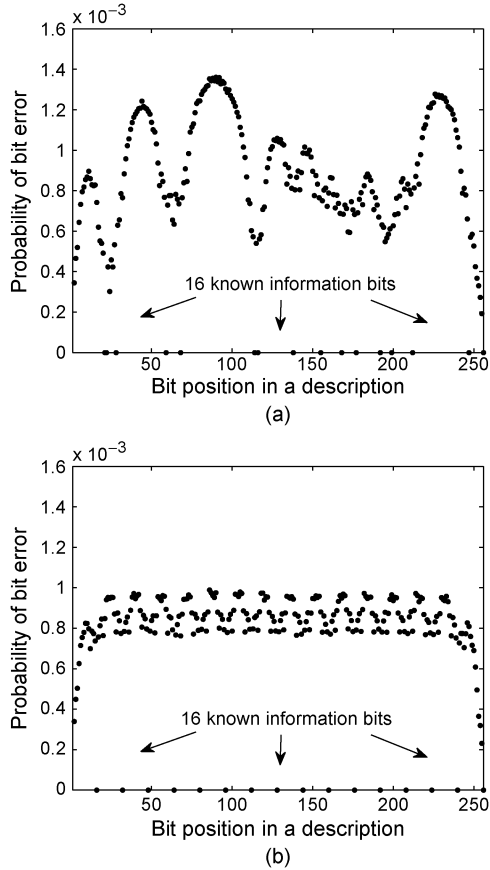


Fig. 5. Probability of bit errors at each position in a description (packet). (a) Sixteen known information bits, which are dispersed in a random manner, are known to the Viterbi algorithm. (b) Sixteen known information bits, which are dispersed by the interleaver, are known to the Viterbi algorithm.

information bits, i.e., the results of RS decoding, will be placed contiguously at the left in a description.

We consider a block interleaver with a specific interrow permutation pattern as the outer interleaver. The interleaving depth and the permutation pattern are designed such that known correct information bits are dispersed uniformly over a description. The input bit sequence to the interleaver is denoted by $b_1, b_2, \dots, b_{LN_{rs}}$, and the output bit sequence from the interleaver is denoted by $y_1, y_2, \dots, y_{LN_{rs}}$. The output sequence is derived as follows.

- 1) The block interleaver depth is set to L , which is the description size in terms of RS code symbols. We assume that L is in the form of $L = 2^i$ ($i \geq 1$ is an integer).
 - 2) Given L , the interrow permutation pattern, which is characterized by vector \mathbf{r}_L , is calculated from the following equations:

$$\text{i) } \mathbf{r}_2 = [1 \ 2] \\ \text{ii) } \mathbf{r}_k = [\mathbf{r}_{k,1} \ \mathbf{r}_{k,2}], \mathbf{r}_{k,1} = 2\mathbf{r}_{k/2}, \mathbf{r}_{k,2} = 2\mathbf{r}_{k/2} - \mathbf{1}_{k/2} \quad (4)$$

where $\mathbf{1}_n$ is an n -tuple all-one vector and $k = 4, 8, 16, \dots, L$.

- 3) Write the input bit sequence into an $L \times N_{\text{rs}}$ matrix row by row, starting with b_1 in the first column of the first row and ending with $b_{LN_{\text{rs}}}$ in the last column of the last row (i.e., the N_{rs} th column of the L th row).

b_1	b_2	b_3	b_4
b_5	b_6	b_7	b_8
b_9	b_{10}	b_{11}	b_{12}
b_{13}	b_{14}	b_{15}	b_{16}
b_{17}	b_{18}	b_{19}	b_{20}
b_{21}	b_{22}	b_{23}	b_{24}
b_{25}	b_{26}	b_{27}	b_{28}
b_{29}	b_{30}	b_{31}	b_{32}

Fig. 6. $L \times N_{rs}$ matrices that store input bit sequences in steps 3 and 4. (a) Step 3: Input bits are written row by row. (b) Step 4: Rows are permuted.

- 4) Perform the interrow permutation based on pattern $\mathbf{r}_L = [\mathbf{r}_L(1) \mathbf{r}_L(2) \cdots \mathbf{r}_L(L)]$, where $\mathbf{r}_L(i)$ denotes the i th component of \mathbf{r}_L , and it indicates the new row position of the original i th row after rows are permuted. For example, the second row moves to the $\mathbf{r}_L(2)$ th row as a result of the permutation.
 - 5) Read the output bit sequence $y_1, y_2, \dots, y_{LN_{\text{rs}}}$ column by column from the interrow permuted $L \times N_{\text{rs}}$ matrix. The y_1 corresponds to the first row of the first column, and $y_{LN_{\text{rs}}}$ corresponds to the last row of the last column (i.e., the L th row of the N_{rs} th column).

From step 3), we have N_{rs} input bits in each row. Consider the adjacent input bits b_i and b_{i+1} that are in the same row. Since the interleaving depth is set to L , the interval between b_i and b_{i+1} will be L after they are interleaved in step 5), that is, N_{rs} input bits in the same row are interleaved such that the interval between the adjacent input bits becomes L , and the end-to-end interval between the leftmost and rightmost input bits will be

$$N_{\text{rs}}(L - 1). \quad (5)$$

Note that an RS code symbol consists of N_{rs} bits. From step 3, when only one RS codeword is correctly decoded, all the correct information bits (i.e., N_{rs} bits) would be written in a single row. In addition, note that the number of information bits in a convolutional code (or a description) is $N_{\text{rs}}L$. Therefore, even when a single RS codeword is correctly decoded, from (5), correct information bits will be interleaved uniformly over a description because the interleaving depth was chosen as L . On the other hand, the interrow permutation pattern suggested in step 2 is related to the distribution of the interleaved bits when more than one RS codeword is correctly decoded. As an example, consider $N_{\text{rs}} = 4$ and $L = 8$. From steps 1 and 2, the interleaver depth is set to 8, and the interrow permutation pattern is given by

$$\mathbf{r}_8 = [4 \ 8 \ 2 \ 6 \ 3 \ 7 \ 1 \ 5] \quad (6)$$

which follows from $\mathbf{r}_2 = [1 \ 2]$ and $\mathbf{r}_4 = [2 \ 4 \ 1 \ 3]$. Fig. 6(a) and (b) depicts $L \times N_{rs}$ matrices, which store input bit sequences after steps 3 and 4 are performed, respectively. The interrow permutation pattern given by (6) was used to generate the matrix in Fig. 6(b). Fig. 7 depicts the positions

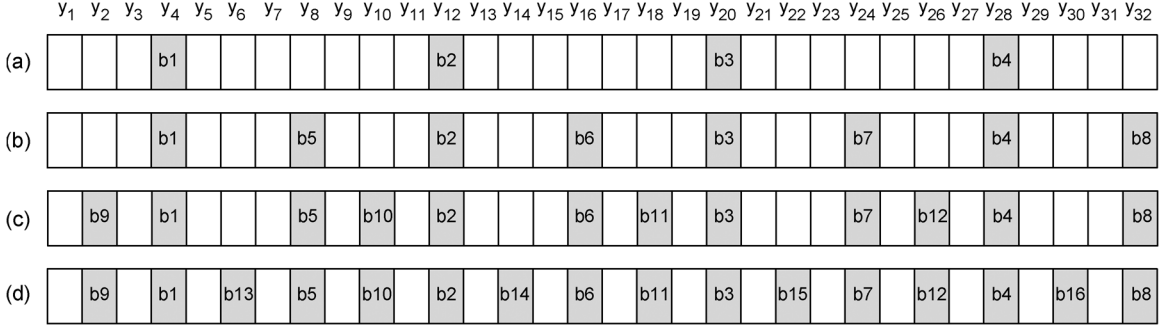


Fig. 7. Positions of known correct information bits in a description.

of known correct information bits in a description after they are interleaved according to steps 1–5. The shaded small boxes denote known correct information bits. Subfigures (a), (b), (c), and (d) indicate the cases when the numbers of correct RS codewords are 1, 2, 3, and 4, respectively (i.e., $C = 1, 2, 3, 4$). That is, the numbers of known correct information bits are 4, 8, 12, and 16, respectively (i.e., $CN_{rs} = 4, 8, 12, 16$). As shown in Fig. 7(c), for some numbers of correct RS codewords, the known correct information bits are dispersed only approximately uniformly. This is because the encoder does not know how many RS codewords will be correctly decoded at the receiver, and thus the interleaving pattern cannot be adapted to a specific number of known correct information bits.

Fig. 5(b) depicts the probability of bit errors at each position in a convolutional code (or description), when 16 known correct information bits are dispersed following the above steps. Compared with the cases in Figs. 4(a) and 5(a), more decoded bits show improved error probabilities, and the maximal error probability in a description is reduced. Fig. 8 depicts the resultant probability of erasures (i.e., the probability of description errors) at various SNRs. Decoding scheme II with the outer interleaver considerably reduces the probability of erasures, compared with decoding scheme I. In Fig. 8(a) and (b), it is also shown that as more correct information bits are available to the Viterbi algorithm, better decoding capability can be achieved.

IV. OPTIMIZATION OF RS CODE PARITY LEVEL FOR UNEQUAL ERROR PROTECTION IN ITERATIVE DECODING

Here, we present the optimal allotment of parity symbols to RS codewords in iterative decoding. Determining RS code parity levels, which involves unequal error protection shown in Fig. 1, is a key design problem of multiple description codes to improve the system performance [11], [16], [17], [19]. There are numerous optimization algorithms [11], [14]–[16], [40], [41], and all of these require that the optimizer knows the probability distribution of the number of correct descriptions at the receiver. This is because, for a given RS parity level, the average distortion of the source can be calculated from both the probability distribution and the rate–distortion curve of the source; during the optimization process, various RS parity levels are compared in terms of the average distortion.

For noniterative decoding, the probability distribution is determined by the channel environment. For iterative decoding, however, the number of correct descriptions possibly increases

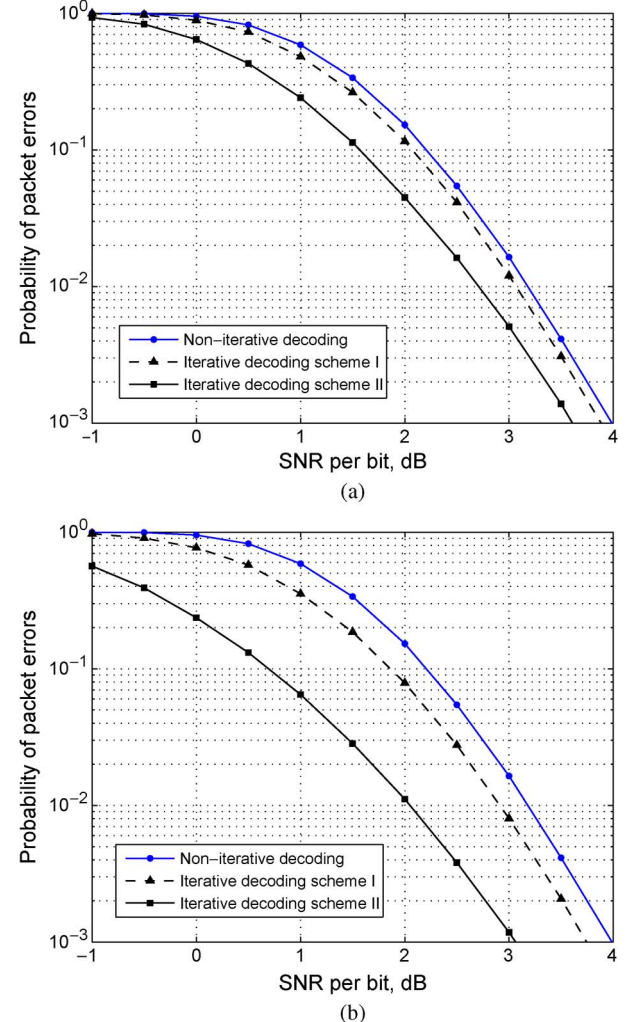


Fig. 8. Probability of description (packet) errors. (a) The number of correct RS codewords is 8 ($C = 8$), i.e., the number of known information bits is 64 ($CN_{rs} = 64$). (b) The number of correct RS codewords is 16 ($C = 16$), i.e., the number of known information bits is 128 ($CN_{rs} = 128$).

after each iteration of decoding, which makes the estimation of the probability distribution more complicated. Note that the increase in correct descriptions depends on how many RS codewords were correctly decoded in the previous iteration because they are exploited as known correct information bits by the Viterbi algorithm. The number of RS codewords, which were correctly decoded in the previous iteration, is determined

by the RS code parity levels in use. Consequently, in iterative decoding, the probability distribution of the correct descriptions is affected by the RS parity levels, which are set up by the encoder. From the facts that the probability distribution depends on RS parity levels and that typically a large number of RS parity levels are compared during the optimization, it follows that a large number of probability distributions should be estimated at the receiver and should be known to the optimizer. Note that the number of possible RS parity levels exponentially increases as the size of the product code increases. Instead of estimating all of them to be used in the optimization, we suggest a method from which the probability distribution for any arbitrary RS parity level can be calculated by combining a set of basis probability profiles.

Let random variables I_k and C_k denote the number of correct descriptions and the number of correct RS codewords at the k th iteration of decoding, respectively ($k \geq 1$). The probability distribution of I_j ($j \geq 2$), denoted by $P_{I_j}(i_j)$, will be derived in the following. From the law of total probability, $P_{I_j}(i_j)$ ($0 \leq i_j \leq N_s$) can be expressed as

$$P_{I_j}(i_j) = \sum_{i_1=0}^{N_s} \sum_{i_2=0}^{N_s} \cdots \sum_{i_{j-1}=0}^{N_s} \sum_{c_1=0}^L \sum_{c_2=0}^L \cdots \sum_{c_{j-1}=0}^L \\ \times P_{I_j|I_{j-1},C_{j-1}}(i_j|\mathbf{i}_{j-1}, \mathbf{c}_{j-1}) P_{\mathbf{I}_{j-1},\mathbf{C}_{j-1}}(\mathbf{i}_{j-1}, \mathbf{c}_{j-1}) \quad (7)$$

where $\mathbf{I}_{j-1} = (I_1, I_2, \dots, I_{j-1})$, $\mathbf{C}_{j-1} = (C_1, C_2, \dots, C_{j-1})$, $\mathbf{i}_{j-1} = (i_1, i_2, \dots, i_{j-1})$, and $\mathbf{c}_{j-1} = (c_1, c_2, \dots, c_{j-1})$. $P_{\mathbf{I}_{j-1},\mathbf{C}_{j-1}}(\mathbf{i}_{j-1}, \mathbf{c}_{j-1})$ is the joint probability distribution of \mathbf{I}_{j-1} and \mathbf{C}_{j-1} , and $P_{I_j|I_{j-1},C_{j-1}}(i_j|\mathbf{i}_{j-1}, \mathbf{c}_{j-1})$ is the conditional probability distribution of I_j given $\mathbf{I}_{j-1} = \mathbf{i}_{j-1}$ and $\mathbf{C}_{j-1} = \mathbf{c}_{j-1}$. Note that the number of correctly decoded RS codewords at the k th iteration C_k is uniquely determined by the number of correct descriptions at the k th iteration, I_k , for a given RS parity level $\mathbf{p} = [p_1 p_2 \cdots p_L]$, where $p_l = N_s - r_l$ is the number of parity symbols assigned to the RS codeword l . That is, the random variable C_k can be expressed as a function of the random variable I_k and a deterministic RS parity level \mathbf{p}

$$C_k = f(I_k, \mathbf{p}), \quad k \geq 1. \quad (8)$$

From (8), $\mathbf{C}_{j-1} = (C_1, C_2, \dots, C_{j-1})$ can be expressed as

$$\mathbf{C}_{j-1} = g(\mathbf{I}_{j-1}, \mathbf{p}) \triangleq (f(I_1, \mathbf{p}), f(I_2, \mathbf{p}), \dots, f(I_{j-1}, \mathbf{p})). \quad (9)$$

From (9), if any component c_k ($1 \leq k \leq j-1$) of $\mathbf{c}_{j-1} = (c_1, c_2, \dots, c_{j-1})$ does not satisfy

$$c_k = f(i_k, \mathbf{p}) \quad (10)$$

we have

$$P_{\mathbf{I}_{j-1},\mathbf{C}_{j-1}}(\mathbf{i}_{j-1}, \mathbf{c}_{j-1}) = 0. \quad (11)$$

From (9) and (11), $P_{I_j}(i_j)$, given by (7), can be rewritten as

$$P_{I_j}(i_j) = \sum_{i_1=0}^{N_s} \sum_{i_2=0}^{N_s} \cdots \sum_{i_{j-1}=0}^{N_s} P_{I_j|I_{j-1},\mathbf{C}_{j-1}}(i_j|\mathbf{i}_{j-1}, g(\mathbf{i}_{j-1}, \mathbf{p})) \\ \times P_{\mathbf{I}_{j-1},\mathbf{C}_{j-1}}(\mathbf{i}_{j-1}, g(\mathbf{i}_{j-1}, \mathbf{p})) \quad (12)$$

for $0 \leq i_j \leq N_s$. From (9), we have the second equality in the following:

$$\begin{aligned} & P_{\mathbf{I}_{j-1},\mathbf{C}_{j-1}}(\mathbf{i}_{j-1}, g(\mathbf{i}_{j-1}, \mathbf{p})) \\ &= P_{\mathbf{I}_{j-1}|\mathbf{C}_{j-1}}(\mathbf{i}_{j-1}|g(\mathbf{i}_{j-1}, \mathbf{p})) P_{\mathbf{C}_{j-1}}(g(\mathbf{i}_{j-1}, \mathbf{p})) \\ &= P_{\mathbf{I}_{j-1}|\mathbf{C}_{j-1}}(\mathbf{i}_{j-1}|g(\mathbf{i}_{j-1}, \mathbf{p})). \end{aligned} \quad (13)$$

From (12), (13), and the chain rule, the probability distribution at the j th iteration $P_{I_j}(i_j)$ can be expressed as

$$P_{I_j}(i_j) = \sum_{i_1=0}^{N_s} \sum_{i_2=0}^{N_s} \cdots \sum_{i_{j-1}=0}^{N_s} P_{\mathbf{I}_j|\mathbf{C}_{j-1}}(\mathbf{i}_j|g(\mathbf{i}_{j-1}, \mathbf{p})) \quad (14)$$

where $P_{\mathbf{I}_j|\mathbf{C}_{j-1}}(\mathbf{i}_j|\mathbf{c}_{j-1})$ is the conditional joint probability distribution of $\mathbf{I}_j = (I_1, I_2, \dots, I_j)$ given $\mathbf{C}_{j-1} = \mathbf{c}_{j-1}$. As an example, from (14), the probability distribution at the second iteration of decoding $P_{I_2}(i_2)$ can be expressed as

$$P_{I_2}(i_2) = \sum_{i_1=0}^{N_s} P_{I_1,I_2|C_1}(i_1, i_2|f(i_1, \mathbf{p})), \quad 0 \leq i_2 \leq N_s \quad (15)$$

where $P_{I_1,I_2|C_1}(i_1, i_2|c_1)$ is the conditional joint probability distribution of I_1 and I_2 , given $C_1 = c_1$. Equation (15) indicates that from a set of only $L+1$ basis probability profiles of $P_{I_1,I_2|C_1}(i_1, i_2|c_1)$ ($c_1 = 0, 1, \dots, L$), which are estimated at the receiver, we can arbitrarily generate the probability distribution at the second iteration $P_{I_2}(i_2)$ for any given RS parity level \mathbf{p} that can be chosen among N_s^L possible ones (note that N_s is the number of possible parity symbols for each RS codeword, and L is the number of RS codewords in the multiple description codes shown in Fig. 1). As a result, with no need to estimate the probability distribution for each RS parity level, a large number of RS parity levels can be compared during the optimization process so as to realize the optimal unequal error protection. Lastly, we note that once the parity level is determined, it should be known to both the receiver and the transmitter before the data are transmitted. Clearly, once the data are transmitted, the parity level cannot be altered while the receiver performs iterative decoding. Hence, the parity level should be optimized to maximize the performance at the final iteration of decoding, based on the iterative decoding capability of the receiver.

V. NUMERICAL EVALUATION AND DISCUSSION

We evaluate the performance of the proposed iterative decoding algorithms. The proposed decoding scheme is a general one that can be used in any multiple description coding system. In this section, as an example application, the performance is evaluated over an OFDM system [17]–[19], [25]–[27]. The standard 8-bits-per-pixel (bpp) 128 × 128 Lena image is transmitted with a rate of 2 bpp, using the progressive source coder SPIHT [2]. To find the optimal allocation of RS parity symbols, we use the popular hill climbing optimization approach proposed in [11]. This algorithm was widely adopted [17]–[19], [25] and described in [11, Section IV] in detail. The number of parity symbols for the RS codeword l ($1 \leq l \leq L$), $N_s - r_l$ is optimized according to the procedure shown in [11, Fig. 5]. As stated in Section IV, the average distortions for various RS

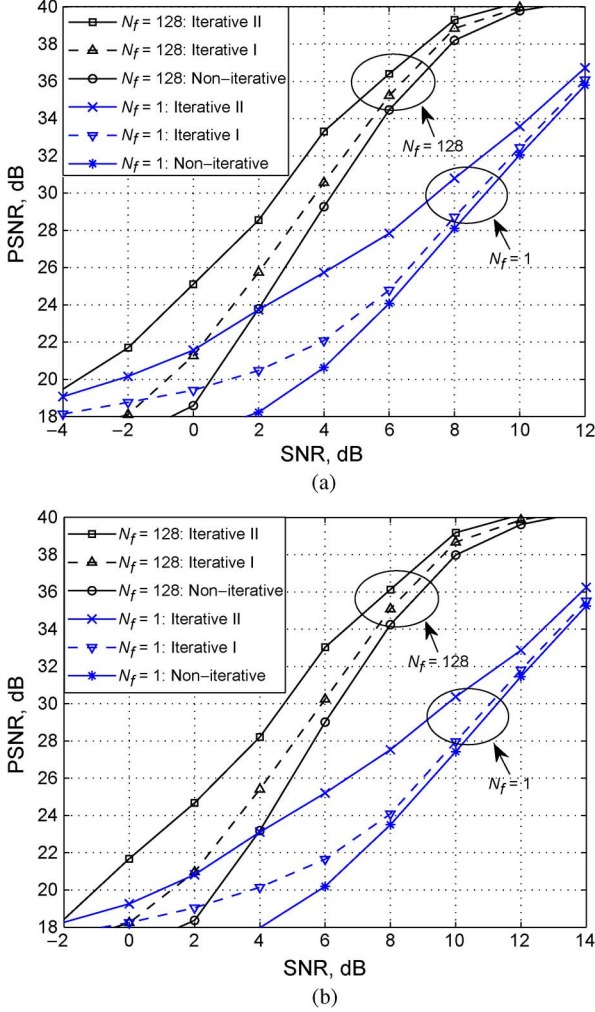


Fig. 9. PSNR performance of iterative decoding schemes I and II at the second iteration. A fast fading channel with a normalized Doppler frequency of 0.031 ($N_t = 8$) is used. (a) Perfect CSI at the receiver. (b) Imperfect CSI at the receiver.

parity levels should be computed and compared during the optimization process (see line 15 of [11, Fig. 5]). Let $D(x)$ denote the operational rate-distortion curve of the source, and let $D(0)$ denote the distortion when the decoder reconstructs the source with no received information. It can be shown that the average distortion, denoted by $E[D]$, is given by

$$E[D] = D(0)Pr(0) + \sum_{l=1}^L \left\{ D \left(\sum_{k=1}^l N_{rs} r_k \right) Pr \left(\sum_{k=1}^l N_{rs} r_k \right) \right\} \quad (16)$$

where $Pr(R)$ is the probability that the system throughput in terms of source progressive bits is R . It can be shown that $E[D]$ is expressed as

$$E[D] = D(0) \sum_{i=0}^{r_1-1} P_I(i) + \sum_{l=1}^L \left\{ D \left(\sum_{k=1}^l N_{rs} r_k \right) \sum_{i=r_l}^{r_{l+1}-1} P_I(i) \right\} \quad (17)$$

where $P_I(i)$ denotes the probability that the number of correct descriptions is i , and we define $\sum_{i=i_1}^{i_2} f(i) \equiv 0$ for $i_2 < i_1$ for any function $f(i)$, and $r_{L+1} \equiv N_s + 1$.

To find the optimal RS parity level at the j th iteration of decoding, the average distortions for various RS parity levels at the j th iteration should be computed. For this computation, (14) and (17) will be used. As the simplest case of iterative decoding, we evaluate the performance at the second iteration: $P_{I_2}(i_2)$ given by (15) is substituted into $P_I(i)$ in (17) to obtain $E[D]$. The resultant expected distortion $E[D]$ is converted into peak-signal-to-noise ratio (PSNR) using $PSNR = 10 \log(255^2/E[D])$. An RS code symbol consists of 8 bits (i.e., $N_{rs} = 8$), the description size is 32 RS code symbols (i.e., $L = 32$), and the convolutional code specified in Section III is employed. It is assumed that any bit errors in a description can be detected by the CRC decoder such that all the erroneous descriptions can be treated as erasures. That is, a perfect CRC code is assumed. Regarding the OFDM system, the number of subcarriers $N_s = 128$, and the modulation is QPSK. The block fading channel model is used in the frequency domain, where the number of independent subbands is 1, 2, 16, and 128 (i.e., $N_f = 1, 2, 16, 128$). In the time domain, we also assume block fading with N_t independent fading components during the time period of one OFDM frame. The performance is evaluated for a slow fading channel with $N_t = 2$ and a fast fading channel with $N_t = 8$, which correspond to normalized Doppler frequencies of about 0.0076 and 0.031, respectively. The normalized Doppler frequency is defined as the number of independent fading components during one modulation symbol period. We assume that perfect channel state information (CSI) is available at the receiver for the slow fading channel. For fast fading, the PSNR performance is evaluated for both cases of perfect and imperfect CSI at the receiver. For imperfect CSI, we use the popular additive channel estimation error model described in [42] as follows:

$$\hat{\alpha}[n, u, v] = \alpha[n, u, v] + q[n, u, v] \quad (18)$$

where $\hat{\alpha}[n, u, v]$ is the estimate of the channel coefficient, $\alpha[n, u, v]$ is given in (1), and $q[n, u, v]$ is a complex Gaussian random variable, which is independent of $\alpha[n, u, v]$, with a zero mean and variance σ_q^2 . We rewrite the output signal $r[n, u, v]$ given by (1) as

$$r[n, u, v] = \alpha[n, u, v]s[n, u, v] + w[n, u, v] \quad \text{for } 1 \leq n \leq N_f, 1 \leq u \leq M, 1 \leq v \leq V. \quad (19)$$

We denote the variances of $s[n, u, v]$ and $w[n, u, v]$ by σ_s^2 and σ_w^2 , respectively. We assume that $|\alpha[n, u, v]|^2/\sigma_q^2$ is proportional to $|\alpha[n, u, v]|^2\sigma_s^2/\sigma_w^2$ (i.e., $\sigma_q^2 = k \cdot \sigma_w^2/\sigma_s^2$, where k is a constant). That is, we assume that more accurate CSI is available at the receiver as the channel SNR improves. In the following evaluation, as an example, we set k to be 2. The resultant PSNR performance at the second iteration is depicted in Figs. 9 and 10.

From Figs. 9 and 10, it is seen that iterative decoding scheme II significantly improves the system performance at the second iteration of decoding, and it outperforms decoding scheme I, which is consistent with the results presented in Section III. We have similar results for $N_f = 2$ and 16. In Fig. 9(a) and (b),

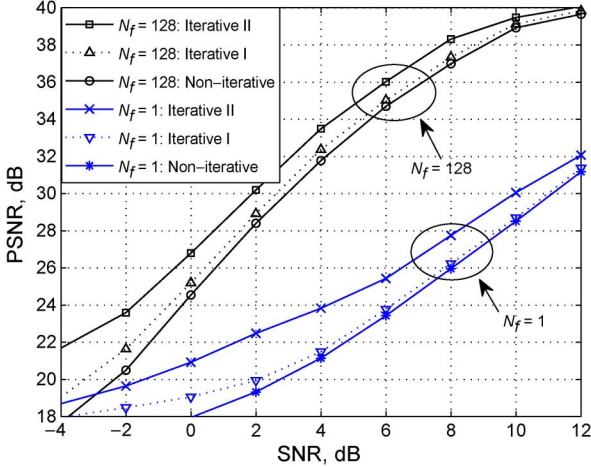


Fig. 10. PSNR performance of iterative decoding schemes I and II at the second iteration. A slow fading channel with a normalized Doppler frequency of 0.0076 ($N_t = 2$) is used. Perfect CSI at the receiver is assumed.

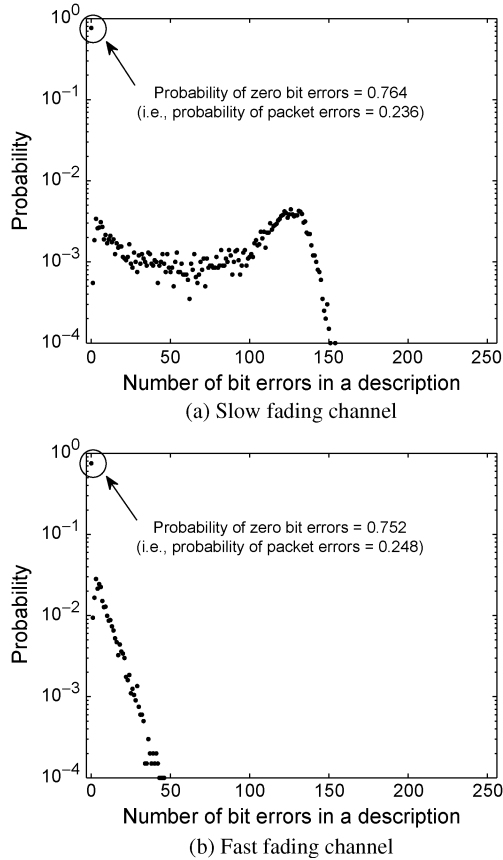


Fig. 11. Probability distribution of the number of bit errors in a description (packet). (a) Rayleigh fading coefficients in the time domain are constant over a description (i.e., extremely slow fading channel). Perfect CSI at the receiver is assumed. SNR is 7 dB, and the probability of zero bit errors is 0.764 (i.e., probability of packet errors is 0.236). (b) Rayleigh fading coefficients in the time domain change every modulation symbol (i.e., extremely fast fading channel). Imperfect CSI at the receiver is assumed. SNR is 7 dB, and the probability of zero bit errors is 0.752 (i.e., probability of packet errors is 0.248).

The performances of both noniterative and iterative decoding schemes are degraded with imperfect CSI at the receiver (i.e., both schemes exhibit a channel SNR loss of about 2 dB). Compared with the noniterative decoding scheme, however, iterative decoding scheme II provides much better performance for both

the cases of perfect as well as imperfect CSI at the receiver (i.e., at PSNRs around 30 dB, decoding scheme II achieves a PSNR gain of about 4 dB and 2 dB for $N_f = 128$ and 1, respectively).

Interestingly, from the PSNR curves in Figs. 9 and 10, we observe that iterative decoding offers greater performance improvement in a fast fading channel than it does in a slow fading channel. Consider an extremely slow fading channel where Rayleigh fading coefficients are nearly constant over a description. Then, the modulated symbols in a description have an identical instantaneous SNR, which has a chi-square probability density function with two degrees of freedom (i.e., exponential distribution). The probability density function is given by

$$p(x) = \frac{1}{\gamma_s} e^{-\frac{x}{\gamma_s}}, \quad x > 0 \quad (20)$$

where γ_s is the average SNR. Fig. 11(a) shows the probability distribution of the number of bit errors in a description, when all the modulated symbols have the same instantaneous SNR of exponential distribution of (20). Note that the number of information bits in a description (or convolutional code) is 256, and the horizontal axis denotes the number of bit errors in the range of 1 to 256 bits.² It is seen that an erroneous description is most likely to have a large number of bit errors, i.e., 128 bit errors. Next, consider an extremely fast fading channel where the Rayleigh fading coefficients are independently drawn in every modulated symbol, i.e., all the modulated symbols have independent instantaneous SNRs of exponential distribution. For this channel, in the case of imperfect CSI at the receiver, the probability distribution of the number of bit errors in a description is depicted in Fig. 11(b).

We compare the probability distributions in Fig. 11(a) and (b). The probabilities of description errors are roughly identical (0.236 and 0.248). Hence, it is expected that noniterative decoding would perform roughly the same for both fading channels. However, the probability distributions are quite different. For the slow fading channel in Fig. 11(a), an erroneous description is most likely to have 128 bit errors, whereas for the fast fading channel in Fig. 11(b), an erroneous description is likely to have much fewer bit errors. We restate the mechanism by which iterative decoding improves the system performance: From the correctly decoded RS codewords, known correct information bits are provided to the Viterbi algorithm in the subsequent iteration. As a result, some bit errors in erroneous descriptions are possibly corrected; thus, the number of correct descriptions increases. However, if erroneous descriptions contain too many bit errors, those descriptions would not be corrected by the Viterbi algorithm even with known correct information bits. Hence, we expect that an erroneous description in the fast fading channel is more likely to be corrected by iterative decoding than in the slow fading channel. This indicates that iterative decoding can achieve greater performance improvement in fast fading channels. That is, the probability distribution in the fast fading channel is more suitable for performance improvement by iterative decoding. For the slow fading channel in Fig. 11(a), there is no diversity in the time

² Fig. 11(a) shows that there is nonzero probability for the number of bit errors greater than 128 bits, although the bit error probability should be less than or equal to 0.5. This is due to the limited size of a description. If the description size were infinitely long, there would be zero probability for the number of bit errors, which are greater than half the size of a description.

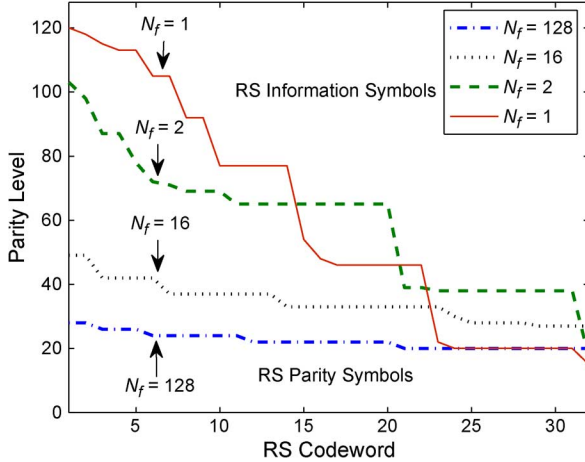


Fig. 12. Optimal allocation of RS parity symbols at the first iteration (i.e., noniterative decoding). SNR is 8 dB, and a fast fading channel with the normalized Doppler frequency of 0.031 ($N_t = 8$) is used. Perfect CSI at the receiver is assumed.

domain. Therefore, when a description fades, it has many bit errors. This can be verified in Fig. 11(a). An erroneous description, which contains such bursty bit errors, is less likely to be corrected. For the fast fading channel, however, a burst of bit errors seldom occurs due to the diversity in the time domain, which can be seen from Fig. 11(b).

Next, we present the optimal RS parity level for iterative decoding whose performance is shown in Figs. 9 and 10. In the first place, Fig. 12 depicts the RS parity level optimized for noniterative decoding. The SNR is 8 dB, and a fast fading channel ($N_t = 8$) is used. Perfect CSI at the receiver is assumed. The symbols above the boundaries are the information symbols for RS codewords, whereas those below the boundaries are the parity symbols. It is seen that fewer parity symbols are added as we move to the right since the relative importance of a progressive bitstream is strictly decreasing. The parity level exhibits stepwise behavior, and the step size becomes greater as $M (= N_s/N_f)$ increases, i.e., N_f decreases. For the block fading channel model, M subcarriers within the same subband are highly correlated; thus, most description errors occur as a bundle of $M, 2M, \dots, N_f M$. This indicates that when deciding the number of RS parity symbols, the optimizer includes M more or M fewer descriptions, instead of including one more or one fewer description, because the correlated nature of subcarriers makes it unlikely that only one more or one fewer description is erroneous. It is also seen that the parity level shows a lower slope as the number of independent subbands N_f increases. Note that, as N_f increases, the number of descriptions having independent fading coefficients increases. This results in a smaller variance of the number of description errors. As a result, we have a smaller gap between the maximum and the minimum number of parity symbols; hence, the RS parity level exhibits a lower slope.

Fig. 13(a) and (b) depicts the optimal RS parity levels at the second iteration of decoding for iterative decoding scheme II, when SNRs are 8 and 4 dB, respectively. The parity levels of $N_f = 2$ and 16 are similar to those of $N_f = 1$ and 128, respectively; thus, they are not depicted here. As shown, the optimal parity level for iterative decoding considerably differs from that

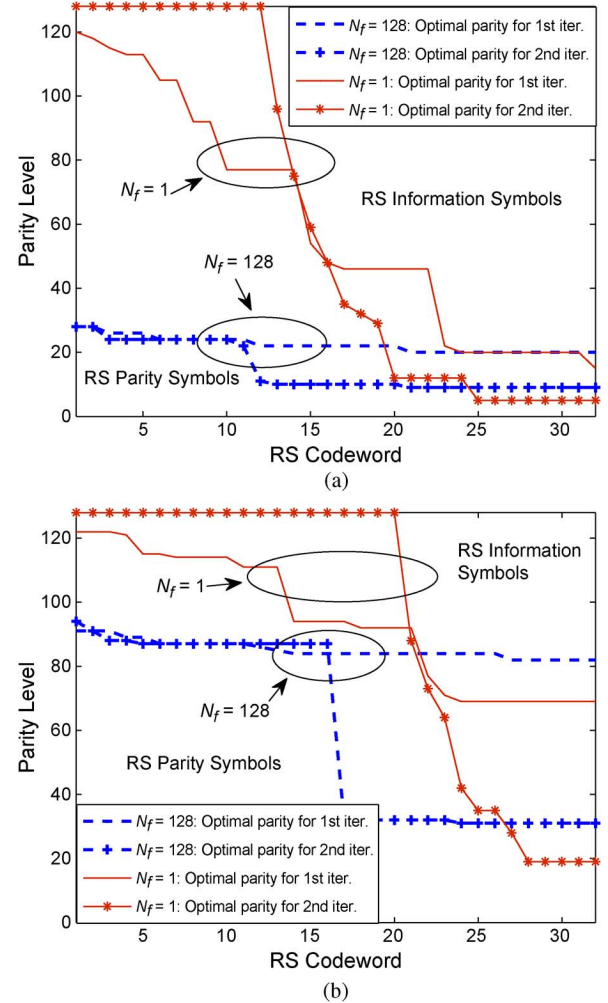


Fig. 13. Optimal allocation of RS parity symbols at the second iteration for iterative decoding scheme II. A fast fading channel with a normalized Doppler frequency of 0.031 ($N_t = 8$) is used. Perfect CSI at the receiver is assumed. (a) SNR = 8 dB. (b) SNR = 4 dB.

for noniterative decoding. To begin with, we consider $N_f = 1$. For the RS codewords at the left, the number of parity symbols for the second iteration is much greater than that for noniterative decoding. However, we have the opposite results for the RS codewords at the right. This will be discussed in the following. We first focus on the RS codewords at the left. Note that iterative decoding can improve the system performance only when the correct information bits are offered to the Viterbi algorithm in the subsequent iteration so that erroneous descriptions may be corrected. In addition, note that those correct information bits are the results of RS decoding in the previous iteration. Unfortunately, for small N_f , it is probable that some OFDM frames have no correct descriptions at the first iteration since a majority of subcarriers are highly correlated. This can be verified in Fig. 14(a), which depicts the probability distribution of the number of correct descriptions at the first iteration. Without correct descriptions, RS codewords cannot be decoded; thus, correct information bits cannot be provided to the Viterbi algorithm in the next iteration. Interestingly, the optimal parity levels for the second iteration in Fig. 13(a) and (b) have the number of parity symbols for RS codewords at the left equal to 128, which

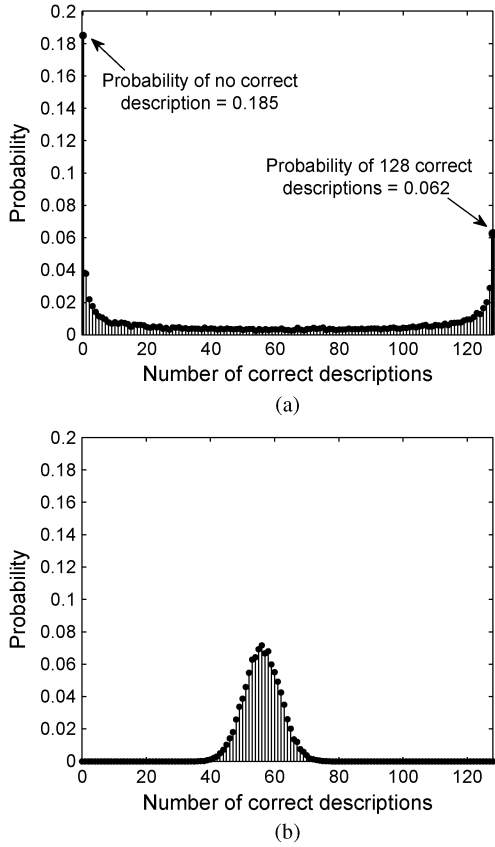


Fig. 14. Probability distribution of the number of correct descriptions (packets) at the first iteration. SNR is 4 dB, and a fast fading channel with a normalized Doppler frequency of 0.031 ($N_t = 8$) is used. Perfect CSI at the receiver is assumed. (a) $N_f = 1$. (b) $N_f = 128$.

is exactly the same as the number of subcarriers. That is, those RS codewords solely consist of predetermined symbols; thus, even without a correct description at the first iteration, known correct information bits can be given to the Viterbi algorithm in the subsequent iteration. It seems that the motivation to allocate so large a number of parity symbols for RS codewords at the left is to reliably provide correct information bits to the Viterbi decoder in the subsequent iteration, so that the number of correct descriptions may increase. Comparing Fig. 13(a) and (b), we see that, at a lower SNR of 4 dB, more RS codewords at the left have the maximum number of parity symbols.

We next consider RS codewords at the right. Note that RS codewords which are decoded at the second iteration would be to the right of the RS codewords which were decoded at the first iteration. This is because there are fewer parity symbols as we move to the right, due to the unequal error protection. At the second iteration, the number of correct descriptions increases; thus, the RS decoder may decode the codewords with fewer parity symbols. As a result, for the RS codewords at the right, the number of parity symbols for the second iteration is smaller than that for the first iteration. This can be seen from Fig. 13(a) and (b). To conclude the discussion of parity levels for small N_f , we note that the optimizer forces the number of parity symbols for RS codewords at the left to be so large such that the number of correct descriptions may increase at the next iteration. On the other hand, the optimizer sets the number of

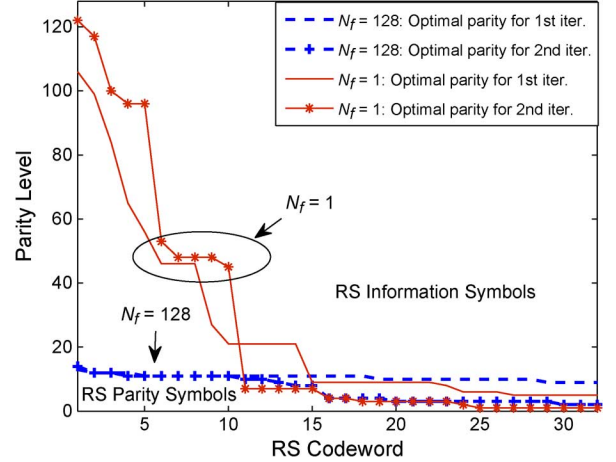


Fig. 15. Optimal allocation of RS parity symbols at the second iteration for iterative decoding scheme II. SNR is 10 dB, and a fast fading channel with a normalized Doppler frequency of 0.031 ($N_t = 8$) is used. Perfect CSI at the receiver is assumed.

parity symbols at the right to be small such that the RS codewords at the right can benefit from the increased number of correct descriptions.

We next consider the case of $N_f = 128$. The difference from the case of $N_f = 1$ is that the number of parity symbols at the left is roughly the same for both noniterative and iterative decoding. For large N_f , a majority of descriptions have independent fading coefficients; thus, it is likely that there always exist some descriptions that are correctly decoded at the first iteration. In addition, as stated before, the variance of the number of correct descriptions is small for large N_f . This can be verified in Fig. 14(b). For $N_f = 128$, the probability that there is no correct description is negligible even at a low SNR of 4 dB. In addition, compared with the case of $N_f = 1$, the variance of the number of correct descriptions is small. As a result, with no need to have so many parity symbols for RS codewords at the left, many known correct information bits can be reliably provided to the Viterbi decoder at the next iteration. On the other hand, RS codewords at the right have fewer parity symbols, such as in the case of $N_f = 1$, since the RS codewords at the right can benefit from the increased number of correct descriptions. This can be seen from Fig. 13(a) and (b). The optimal RS parity levels for the cases of the slow fading channel or the fast fading channel with the imperfect CSI at the receiver also show similar behaviors; thus, they are not presented here.

We observe the RS parity level optimized for iterative decoding when the SNR is high. At a high SNR, even for small N_f , which makes a majority of subcarriers highly correlated, it is unlikely that there exist OFDM frames with no correct descriptions at the first iteration, i.e., the probability of receiving zero correct descriptions is negligible.³ Hence, even for small N_f , it may be inefficient to allocate so many parity symbols for the RS codewords at the left. This can be seen from Fig. 15. For $N_f = 1$, the number of parity symbols for iterative decoding is much less than 128 symbols in most RS codewords at the left. This differs from the cases of lower SNRs shown in Fig. 13(a) and (b). On the other hand, at a high SNR, many

³This can be verified from the probability distribution of the number of correct descriptions at high SNR, which is not depicted here for limited space.

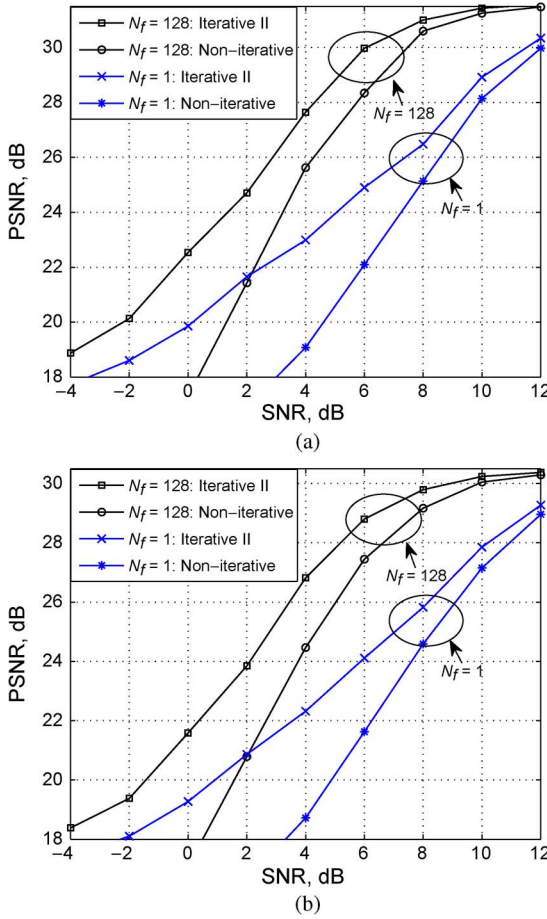


Fig. 16. PSNR performance of iterative decoding scheme I at the second iteration. A fast fading channel with normalized Doppler frequency of 0.031 ($N_t = 8$) is used. Perfect CSI at the receiver is assumed. (a) Pepper image with a rate of 0.5 bpp. (b) Cameraman image with a rate of 0.5 bpp.

descriptions are correctly decoded at the first iteration for both large and small N_f values.³ Hence, there is a slight room for the number of correct descriptions to be increased in the subsequent iteration; thus, the optimizer can reduce only a limited number of parity symbols for RS codewords at the right. This can be seen from Fig. 15 for both the cases of $N_f = 1$ and 128, which differs from the cases of lower SNRs shown in Fig. 13(a) and (b). For these reasons, when SNR is high, the parity level optimized for iterative decoding does not make a significant difference from that for noniterative decoding.

Lastly, we observe the performance for the transmission of other images such as Pepper and Cameraman, each with a rate of 0.5 bits per pixel. The results are given in Fig. 16. In Figs. 9(a) and 16(a) and (b), it is shown that the maximum achievable PSNR depends on both the bpp as well as the image employed in the system. However, for all of the above cases, the proposed iterative decoder significantly improves the system performance.

VI. CONCLUSION

Recently, multiple description coding has emerged as an attractive framework for robust multimedia transmission over wireless/wired networks. In this paper, we have proposed novel iterative decoding algorithms of FEC-based multiple description codes. Once a decoded description is declared an

erasure, the entire description is abandoned for RS erasure decoding. However, if some bit errors can be corrected, the description might be used to enhance the decoding capability of RS erasure codes. This gives the motivation to address the iterative decoding of multiple description codes. Our proposed decoding algorithms take advantage of the error detection capability of RS codes. The correctly decoded hard-decision results of systematic RS decoding are given to the Viterbi algorithm as known correct information bits in the next iteration of decoding. An important feature of the proposed algorithm is the use of an intradescription interleaver, which distributes the hard-decision results of RS codewords uniformly over a description such that the Viterbi decoder can achieve fewer description erasures at the next iteration. A specific interrow permutation pattern and the interleaving depth were suggested. The suggested interleaver does not affect the performance of noniterative decoding but significantly enhances the performance when the system is iteratively decoded.

For unequal error protection, i.e., a key design issue in progressive transmission systems, we addressed the optimal allotment of parity symbols to RS codewords. There are numerous algorithms for the optimization of RS parity levels in multiple description codes, but these require that the probability distribution of the number of erasures should be known to the optimizer. In iterative decoding, however, it is more complicated to estimate all the required probability distributions. We derived the mathematical equations by which the probability distributions can be generated in a simple way from a set of basis probability profiles; therefore, the estimation of a large number of probability distributions can be avoided at the receiver. The performance of the proposed decoding schemes was evaluated for multiple description codes in a wireless OFDM system. The numerical results showed that the PSNR performance of FEC-based multiple description codes can be significantly improved if the proposed iterative decoding algorithm is applied, and the RS parity level is optimized for unequal error protection based on our method. We also presented technical discussions on how the coherence time in OFDM frames affects the performance of iterative decoding. Lastly, some discussions were given on the singular behaviors exhibited by RS code parity levels optimized for iterative decoding.

REFERENCES

- [1] Y. Shen, P. C. Cosman, and L. B. Milstein, "Video coding with fixed length packetization for a tandem channel," *IEEE Trans. Image Process.*, vol. 15, no. 2, pp. 273–288, Feb. 2006.
- [2] A. Said and W. A. Pearlman, "A new, fast, and efficient image codec based on set partitioning in hierarchical trees," *IEEE Trans. Circuits Syst. Video Technol.*, vol. 6, no. 3, pp. 243–250, Jun. 1996.
- [3] D. Taubman and M. Marcellin, *JPEG2000: Image Compression Fundamentals, Standards, and Practice*. Norwell, MA: Kluwer, 2001.
- [4] H. Schwarz, D. Marpe, and T. Wiegand, "Overview of the scalable video coding extension of H.264/AVC," *IEEE Trans. Circuits Syst. Video Technol.*, vol. 17, no. 9, pp. 1103–1120, Sep. 2007.
- [5] P. G. Sherwood and K. Zeger, "Progressive image coding for noisy channels," *IEEE Signal Process. Lett.*, vol. 4, no. 7, pp. 189–191, Jul. 1997.
- [6] P. Cosman, J. Rogers, P. G. Sherwood, and K. Zeger, "Combined forward error control and packetized zerotree wavelet encoding for transmission of images over varying channels," *IEEE Trans. Image Process.*, vol. 9, no. 6, pp. 982–993, Jun. 2000.
- [7] V. K. Goyal, "Multiple description coding: Compression meets the network," *IEEE Signal Process. Mag.*, vol. 18, no. 5, pp. 74–93, Sep. 2001.

- [8] S. S. Pradhan, R. Puri, and K. Ramchandran, “ n -channel symmetric multiple descriptions—Part I: (n, k) source channel erasure codes,” *IEEE Trans. Inf. Theory*, vol. 50, no. 1, pp. 47–61, Jan. 2004.
- [9] A. E. El Gamal and T. M. Cover, “Achievable rates for multiple descriptions,” *IEEE Trans. Inf. Theory*, vol. IT-28, no. 6, pp. 851–857, Nov. 1982.
- [10] J. K. Wolf, A. D. Wyner, and J. Ziv, “Source coding for multiple descriptions,” *Bell Syst. Tech. J.*, vol. 59, no. 8, pp. 1417–1426, Oct. 1980.
- [11] A. Mohr, E. Riskin, and R. Ladner, “Unequal loss protection: Graceful degradation of image quality over packet erasure channels through forward error correction,” *IEEE J. Sel. Areas Commun.*, vol. 18, no. 6, pp. 819–828, Jun. 2000.
- [12] M. van der Schaar and H. Radha, “Unequal packet loss resilience for fine-granular-scalability video,” *IEEE Trans. Multimedia*, vol. 3, no. 4, pp. 381–394, Dec. 2001.
- [13] A. Albanese, J. Blomer, J. Edmonds, M. Luby, and M. Sudan, “Priority encoded transmission,” *IEEE Trans. Inf. Theory*, vol. 42, no. 6, pp. 1737–1744, Nov. 1996.
- [14] R. Puri, K.-W. Lee, K. Ramchandran, and V. Bharghavan, “An integrated source transcoding and congestion control paradigm for video streaming in the Internet,” *IEEE Trans. Multimedia*, vol. 3, no. 1, pp. 18–32, Mar. 2001.
- [15] R. Puri and K. Ramchandran, “Multiple description source coding using forward error correction codes,” in *Proc. 33rd Asilomar Conf. Signals, Syst., Comput.*, Pacific Grove, CA, Oct. 1999, pp. 342–346.
- [16] D. G. Sachs, R. Anand, and K. Ramchandran, “Wireless image transmission using multiple-description based concatenated codes,” in *Proc. SPIE*, San Jose, CA, Jan. 2000, vol. 3974, pp. 300–311.
- [17] Y. S. Chan, P. C. Cosman, and L. B. Milstein, “A cross-layer diversity technique for multi-carrier OFDM multimedia networks,” *IEEE Trans. Image Process.*, vol. 15, no. 4, pp. 833–847, Apr. 2006.
- [18] Y. S. Chan, P. C. Cosman, and L. B. Milstein, “A multiple description coding and delivery scheme for motion-compensated fine granularity scalable video,” *IEEE Trans. Image Process.*, vol. 17, no. 8, pp. 1353–1367, Aug. 2008.
- [19] L. Toni, Y. S. Chan, P. C. Cosman, and L. B. Milstein, “Channel coding for progressive images in a 2-D time-frequency OFDM block with channel estimation errors,” *IEEE Trans. Image Process.*, vol. 18, no. 11, pp. 2476–2490, Nov. 2009.
- [20] P. G. Sherwood and K. Zeger, “Error protection for progressive image transmission over memoryless and fading channels,” *IEEE Trans. Commun.*, vol. 46, no. 12, pp. 1555–1559, Dec. 1998.
- [21] M. Srinivasan, “Iterative decoding of multiple descriptions,” in *Proc. DCC*, Mar. 1999, pp. 463–472.
- [22] C. Berrou, A. Glavieux, and P. Thitimajshima, “Near Shannon limit error-correcting coding and decoding: Turbo-codes,” in *Proc. IEEE ICC*, May 1993, pp. 1064–1070.
- [23] Y. Sun, Z. Xiong, and X. Wang, “Iterative decoding of differentially space-time coded multiple descriptions of images,” *IEEE Signal Process. Lett.*, vol. 11, no. 8, pp. 686–689, Aug. 2004.
- [24] B. L. Hughes, “Differential space-time modulation,” *IEEE Trans. Inf. Theory*, vol. 46, no. 7, pp. 2567–2578, Nov. 2000.
- [25] S.-S. Tan, M. Rim, P. C. Cosman, and L. B. Milstein, “Adaptive modulation for OFDM-based multiple description progressive image transmission,” in *Proc. IEEE GLOBECOM*, New Orleans, LA, Nov./Dec. 2008, pp. 1–5.
- [26] L. Pu, M. W. Marcellin, I. Djordjevic, B. Vasic, and A. Bilgin, “Joint source-channel rate allocation in parallel channels,” *IEEE Trans. Image Process.*, vol. 16, no. 8, pp. 2016–2022, Aug. 2007.
- [27] S. K. Bandyopadhyay, G. Partasides, and L. P. Kondi, “Cross-layer optimization for video transmission over multirate GMC-CDMA wireless links,” *IEEE Trans. Image Process.*, vol. 17, no. 6, pp. 1020–1024, Jun. 2008.
- [28] R. J. McEliece and W. E. Stark, “Channels with block interference,” *IEEE Trans. Inf. Theory*, vol. IT-30, no. 1, pp. 44–53, Jan. 1984.
- [29] M. Medard and R. G. Gallager, “Bandwidth scaling for fading multipath channels,” *IEEE Trans. Inf. Theory*, vol. 48, no. 4, pp. 840–852, Apr. 2002.
- [30] R. Knopp and P. A. Humblet, “On coding for block fading channels,” *IEEE Trans. Inf. Theory*, vol. 46, no. 1, pp. 189–205, Jan. 2000.
- [31] S. Lin and D. J. Costello, Jr., *Error Control Coding: Fundamentals and Applications*, 2nd ed. Englewood Cliffs, NJ: Prentice-Hall, 2004.
- [32] R. D. Cidecian, E. Eleftheriou, and M. Rupf, “Concatenated Reed-Solomon/convolutional coding for data transmission in CDMA-based cellular systems,” *IEEE Trans. Commun.*, vol. 45, no. 10, pp. 1291–1303, Oct. 1997.
- [33] L.-N. Lee, “Concatenated coding systems employing a unit-memory convolutional code and a byte-oriented decoding algorithm,” *IEEE Trans. Commun.*, vol. COM-25, no. 10, pp. 1064–1074, Oct. 1977.
- [34] O. Aitsab and R. Pyndiah, “Performance of concatenated Reed-Solomon convolutional codes with iterative decoding,” in *Proc. IEEE GLOBECOM*, Phoenix, AZ, Nov. 1997, vol. 2, pp. 934–938.
- [35] S. B. Wicker, *Error Control Systems for Digital Communication and Storage*. Englewood Cliffs, NJ: Prentice-Hall, 1995.
- [36] L. Cao and C. W. Cheng, “A novel product coding and recurrent alternate decoding scheme for image transmission over noisy channels,” *IEEE Trans. Commun.*, vol. 51, no. 9, pp. 1426–1431, Sep. 2003.
- [37] L. Cao and C. W. Cheng, “Constrained SOVA decoding in concatenated codes,” in *Proc. IEEE WCNC*, Mar. 2004, vol. 4, pp. 2280–2284.
- [38] Z. Ting, X. Ming, C. Dong-Xia, and Y. Lun, “Constrained Viterbi algorithm and its application in SPIHT coded images transmission,” in *Proc. IEEE ICOSP*, Nov. 2006.
- [39] J. G. Proakis, *Digital Communication*, 3rd ed. New York: McGraw-Hill, 1995.
- [40] T. Stockhammer and C. Buchner, “Progressive texture video streaming for lossy packet network,” in *Proc. 11th Packet Video Workshop*, Kyongju, Korea, May 2001.
- [41] A. E. Mohr, R. E. Ladner, and E. A. Riskin, “Approximately optimal assignment for unequal loss protection,” in *Proc. Int. Conf. Image Process.*, Sep. 2000, vol. 1, pp. 367–370.
- [42] R. Annavajjal, P. C. Cosman, and L. B. Milstein, “Performance analysis of linear modulation schemes with generalized diversity combining on Rayleigh fading channels with noisy channel estimates,” *IEEE Trans. Inf. Theory*, vol. 53, no. 12, pp. 4701–4727, Dec. 2007.



Seok-Ho Chang (S’07–M’10) received the B.S. and M.S. degrees in electrical engineering from Seoul National University, Seoul, Korea, in 1997 and 1999, respectively, and the Ph.D. degree in electrical engineering from the University of California at San Diego (UCSD), La Jolla, in 2010.

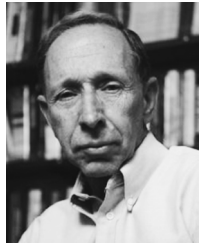
From 1999 to 2005, he was with LG Electronics, Korea, where he was involved in development of WCDMA (3GPP) base/mobile-station modem chips. In 2006, he was with POSCO ICT, Korea, and worked on mobile WiMax systems. From 2010 to 2011, he was with UCSD as a Postdoctoral Scholar, where he was engaged in the cross-layer design of wireless systems. Since 2011, he has been with Qualcomm Inc., San Diego, as a Staff Engineer. His research interests include wireless/wireline digital communication theory, multiple-input multiple-output systems, multiuser information theory, time and frequency synchronization, equalization, and cross-layer design of wireless systems.



Pamela C. Cosman (S’88–M’93–SM’00–F’08) received the B.S. degree (with Honors) from the California Institute of Technology, Pasadena, in 1987, and the M.S. and Ph.D. degrees from Stanford University, Stanford, CA, in 1989 and 1993, respectively, all in electrical engineering.

During 1993–1995, she was an NSF Postdoctoral Fellow with Stanford University and a Visiting Professor with the University of Minnesota, Minneapolis. Since 1995, she has been with the Department of Electrical and Computer Engineering, University of California at San Diego, La Jolla, where she is currently a Professor. From 2006 to 2008, she was the Director of the Center for Wireless Communications. Her research interests include image and video compression and processing, and wireless communications.

Dr. Cosman was a Guest Editor of the June 2000 special issue of the *IEEE Journal on Selected Areas in Communications* on “error-resilient image and video coding” and was the Technical Program Chair of the 1998 Information Theory Workshop in San Diego. She was an Associate Editor of the *IEEE Communications Letters* in 1998–2001 and an Associate Editor of the *IEEE Signal Processing Letters* in 2001–2005. She was the Editor-in-Chief in 2006–2009, as well as a Senior Editor in 2003–2005 and 2010–present, of the *IEEE Journal on Selected Areas in Communications*. She is the recipient of the ECE Departmental Graduate Teaching Award, a Career Award from the National Science Foundation, a Powell Faculty Fellowship, and a Globecom 2008 Best Paper Award. She is a member of Tau Beta Pi and Sigma Xi.



Laurence B. Milstein (S'66–M'68–SM'77–F'85) received the B.E.E. degree from the City College of New York, New York, in 1964, and the M.S. and Ph.D. degrees in electrical engineering from the Polytechnic Institute of Brooklyn, Brooklyn, NY, in 1966 and 1968, respectively.

From 1968 to 1974, he was with the Space and Communications Group, Hughes Aircraft Company, and from 1974 to 1976, he was a member of the Department of Electrical and Systems Engineering, Rensselaer Polytechnic Institute, Troy, NY. Since 1976, he has been with the Department of Electrical and Computer Engineering, University of California, San Diego, San Diego, where he is currently the Ericsson Professor of Wireless Communications Access Techniques and former Department Chair, working in the area of digital communication theory with special emphasis on spread-spectrum communication systems. He has

also been a Consultant to both government and industry in the areas of radar and communications.

Dr. Milstein was an Associate Editor for Communication Theory for the IEEE TRANSACTIONS ON COMMUNICATIONS, an Associate Editor for Book Reviews for the IEEE TRANSACTIONS ON INFORMATION THEORY, an Associate Technical Editor for the *IEEE Communications Magazine*, and the Editor-in-Chief of the IEEE JOURNAL ON SELECTED AREAS IN COMMUNICATIONS. He was the Vice President for Technical Affairs in 1990 and 1991 of the IEEE Communications Society and was the Chair of the IEEE Fellows Selection Committee. He was a recipient of the 1998 Military Communications Conference Long Term Technical Achievement Award, an Academic Senate 1999 UCSD Distinguished Teaching Award, an IEEE Third Millennium Medal in 2000, the 2000 IEEE Communication Society Armstrong Technical Achievement Award, and various prize paper awards, including the 2002 MILCOM Fred Ellersick Award.